1   **Leveraging biological insight and environmental variation to improve phenotypic**

2   **prediction: Integrating crop growth models (CGM) with whole genome prediction (WGP)**

3   C.D Messina*[1], F. Technow[2], T. Tang[1], R. Totir[1], C. Gho[3], M. Cooper[1]

4

5   [1]DuPont Pioneer, 8503 NW 62nd Avenue, Johnston, IA 50131, USA.

6   [2]DuPont Pioneer, 596779 County Road 59N, Woodstock, Ontario N4S 7W1, Canada.

7   [3]DuPont Pioneer, Semillas Pioneer Chile Ltda, Santa Filomena 1609 – Buin, PO Box 267, Chile.

8

9   *Corresponding author:

10 DuPont Pioneer

11 8503 NW 62nd Ave.

12 Johnston, IA 50131

13 USA

14 charlie.messina@pioneer.com

15

16

17

20 **Abstract**

21 A successful strategy for prediction of crop yield that accounts for the effects of genotype and

22 environment will open up many opportunities for enhancing the productivity of agricultural

23 systems. Crop growth models (CGMs) have a history of application for crop management

24 decision support. Recently whole genome prediction (WGP) methodologies have been developed

25 and applied in breeding to enable prediction of crop traits for new genotypes and thus increase the

26 size of plant breeding programs without the need to expand expensive field testing. The presence

27 of Genotype-by-Environment-by-Management (G×E×M) interactions for yield presents a

28 significant challenge for the development of prediction technologies for both product

29 development by breeding and product placement within agricultural production systems. The

30 integration of a CGM into the algorithm for whole genome prediction WGP, referred to as CGM-

31 WGP, has opened up the potential for prediction of G×E×M interactions for breeding and product

32 placement applications. Here a combination of simulation and empirical studies are used to

33 explain how the CGM-WGP methodology works and to demonstrate successful reduction to

34 practice for applications to maize breeding and product placement recommendation in the US

35 corn belt.

36

1. Introduction

Whole Genome Prediction (WGP) is a set of quantitative genetic methodologies that enables prediction of the breeding value of an individual, created from one or more reference populations, based on its genetic makeup and pedigree relations. In combination with high throughput genotyping and phenotyping WGP has brought unprecedented change to the scale of plant breeding (Heffner et al., 2009; Lorenz et al., 2011; Cooper et al., 2014). Unlike the near past, today for most large commercial breeding programs germplasm is evaluated using WGP and only a fraction of the new hybrids that can be created are evaluated in multi-environment trials (MET, Heffner et al., 2009; Cooper et al., 2014). WGP enabled breeders to increase the effective size of their breeding programs without the need to increase the scale of field phenotyping and by doing so accelerated the rate of genetic gain.

The WGP methodology seeks to simultaneously estimate the allelic values at all available polymorphic marker loci across the genome (Meuwissen et al., 2001). Bayesian approaches seek to estimate the posterior distribution of marker effects by means of calculation of a likelihood function and a prior distribution of such effects. This is a data driven process that leverages the availability of large datasets routinely generated in commercial breeding programs. Datasets often comprise multiple years and large samples of genotypes from reference populations with the expectation that these are a representative sample of the germplasm and the target population of environments (TPE, Cooper et al., 2014). The mechanics of the method separates individuals within populations under selection into the WGP estimation set, individuals in this set have both phenotypic and genotypic information, and the prediction set, individuals in this set only have genotypic information (see Heffner et al., 2009, Lorenz et al., 2011). Various statistical methodologies were developed to enable WGP, among which selection of a suitable method depends on genetic architecture of the trait, the ability to demonstrate and model non-linear interactions and the population structure (Lorenz et al., 2011). Recently, the use of biological

62   frameworks to model non-linear genetic effects was advocated to improve prediction accuracy

63   (Marjoram et al., 2014, Technow et al., 2015). A necessary condition to leverage such biological

64   insight in WGP is that that knowledge be encapsulated in the form of quantitative functions that

65   transparently map markers to biological function (Messina et al., 2011; Cooper et al., 2005) and

66   be linked to prediction algorithms (Technow et al., 2015) to generate the necessary boundary

67   conditions to accurately execute the biological algorithms (Cooper et al., 2016).

68   Crop Growth Models (CGMs), structured on principles of resource capture (e.g., solar

69   radiation, water, nitrogen), use efficiency and allocation to organs of economic value, provide the

70   biological framework for phenotypic prediction of relevant quantitative traits for breeding

71   (Cooper et al., 2009). A general mathematical framework to develop models for phenotypic

72   prediction with genetic information based on the E(N:K) family of models (Cooper et al., 2005)

73   has been developed (Messina et al., 2011). Examples of implementations include models of leaf

74   elongation rate and flowering time in maize (Welcker et al., 2007; Dong et al., 2012), and oat and

75   soybean growth and development (Yin et al., 2004; Messina et al., 2006). But the

76   parameterization of CGMs at a scale that is required to support breeding programs using these

77   approaches proved challenging because of the difficulty of phenotyping important physiological

78   traits (Messina et al., 2011). This phenotyping bottleneck currently limits the applicability of

79   CGM to augment plant breeding. Advances in phenomics will undoubtedly generate very large

80   datasets (Furbank and Tester, 2011; Fahlgren et al., 2015) bringing opportunity to improve

81   models, and challenges to the utilization of these sources of information. Efficient analytical

82   methods that reduce the phenotyping requirements and directly integrate biological models, such

83   as CGMs, into the prediction algorithms in a single step, are naturally well positioned to fully

84   take advantage of improvements in phenomics.

85   The CGM-WGP methodology uses a CGM as part of the calculation of the likelihood

86   function step in an otherwise standard WGP algorithm (Technow et al., 2015). The relationship

87   between marker effects and yield is established through the estimation of marker effects and

88   biological parameters within the CGM. Because the selected genetic models result in the

89   modulation of the strength of the relationship between the environment and a physiological

90   process, and/or different physiological processes, genotype-by-environment (G×E), epistasis in

91   the form of trait-by-trait genotype-by-genotype (G×G) and genotype-by-environment-by-

92   management (G×E×M) interactions are all emergent properties from the genetic variation effects

93   in the functional equations that relate traits and the environment (Messina et al., 2011; Cooper et

94   al., 2009). Technow et al (2015) demonstrated this concept using a simulation experiment, while

95   Cooper et al. (2016) demonstrated the feasibility of implementing CGM-WGP within a functional

96   breeding program. However, a demonstration that CGM-WGP prediction accuracy is higher than

97   benchmark methodologies in at least one realistic breeding case study is lacking. It was

98   hypothesized that the difference in predictive accuracy between CGM-WGP and benchmark

99   WGP algorithms will increase with an increasing role of G×E interaction in determination of

100   performance, and that parameterization of the CGM-WGP models will improve with the contrast

101   between environmental conditions (Cooper et al., 2016).

102   Because training of CGM-WGP involves the estimation of biological parameters that

103   regulate physiological behavior, the CGM-WGP not only can output predictions for yield for the

104   set of environments and hybrids used for training as for other prediction methods such as BayesA,

105   but also enables the breeder to exercise the CGM to make predictions to evaluate hybrids that

106   have never been empirically evaluated in the field at a large scale, through computer simulation.

107   This simulation step enables extending predictions from a few G×M or G×E cases intrinsic to the

108   training sets to virtually the target population of environments, here considered broadly to include

109   agronomic practices.

110   The objectives of this paper are to: 1) extend CGM-WGP methodology to train models

111   using data from multiple environments, 2) evaluate, using both synthetic and experimental data

112   from a maize drought breeding program, whether CGM-WGP methodology can enable improved

113   phenotypic prediction when G×E interactions are an important determinant of performance, 3)

114   demonstrate virtual breeding by means of use of CGM-WGP and computer simulation, and 4)

115   facilitate the dialogue between breeders, crop physiologists and modelers.

116

117   **2. Materials and Methods**

118   *2.1 Hierarchical model*

119   The model fitted to the data (Fig. 1) uses the likelihood derived from the generalized

120   E(N:K) model (Cooper et al., 2005; Messina et al. 2011) as,

121
$$y_{ij} \sim N\left(CGM(T_{ti}, E_j), \sigma_{e_j}^2\right)$$

122   where y_{ij} is the yield of individual i in environment j, and T_{ti} is the unobserved value for

123   physiological trait t (e.g., AMAX; a measure of maize canopy size based on the area of the

124   largest leaf) for individual i. The environmental inputs (e.g., soil type, temperature) of

125   environment j are represented by E_j, and $\sigma_{e_j}^2$ denotes the residual variance for yield in that

126   environment. Finally N denotes the Gaussian density function and CGM the crop growth model.

127   Thus, $CGM(T_{ti}, E_j)$ denotes the simulated yield of individual i in environment j, as determined

128   by the states of the physiological traits t for individual i, T_{ti}.

129   The prior for the unobserved T_{ti} was

$$T_{ti} \sim N\left(\beta_{o_t} + \sum_k z_{tik}\, u_{tk}\, , \sigma_{T_t}^2\right)$$

130   where β_{o_t} is a trait specific intercept, z_{tik} denotes the marker score of individual i at marker k for

131   trait t and u_{tk} the effect of marker k for trait t. The trait specific prior variance was $\sigma^2_{T_t}$.

132   The prior distributions for the marker effects correspond to those from the widely used

133   whole genome prediction model 'BayesA' (Meuwissen et al., 2001). Briefly, the marker effects

134   u_{tk} were associated with a Normal prior distribution with mean 0 and marker specific

135   variance σ^2_{tk}, which itself was associated with scaled inverse Chi-square prior distribution with

136   4.001 degrees of freedom and trait specific scaling factor S^2_t. The prior distribution for the

137   parameter S^2_t was a Gamma distribution with constant parameters (Yang and Tempelman, 2012).

138   The prior for the trait specific intercept β_{o_t} was a Normal distribution with mean μ_{0_t} and

139   variance $\sigma^2_{0_t}$, both of which were constants. The prior of $\sigma^2_{T_t}$ was again a scaled inverse Chi

140   square distribution with 4.001 degrees of freedom and constant scaling factor $S^2_{T_t}$. Finally, the

141   prior of the environment specific residual variance $\sigma^2_{e_j}$ was also a scaled inverse chi-square

142   distribution with 4.001 degrees of freedom and constant scaling factor $S^2_{e_j}$. Thus, the CGM-WGP

143   model can be understood as a generalized linear model version of the whole genome prediction

144   model 'BayesA' (Meuwissen et al., 2001), in which the crop growth model acts as the link

145   function.

146   The constants were derived from rough prior estimates of the mean (m_t) and variance

147   (v_t) of physiological trait t within the germplasm under consideration. From these, the scaling

148   factor of the prior of the physiological traits was calculated as $S^2_{T_t} = v_t \cdot (4.001 - 2)/4.001$,

149   which results in a scaled inverse chi-square prior distribution with mean v_t. The prior parameters

150   for the trait specific intercepts β_{o_t} were $\mu_{0_t} = m_t$ and $\sigma^2_{0_t} = v_t$. The parameters of the Gamma

151   prior distribution of S^2_t, the scaling factor of the marker specific variances, were calculated as

152   follows. First the variance of the additive effect of a random marker locus was calculated

153 according to Habier et al. (2011) as $v_{u_t} = v_t / \sum_k 2p_k(1 - p_k)$, where p_k is the allele frequency

154 of marker k. From this we calculated the prior expected value of S_t^2 as $E[S_t^2] = v_{u_t} \cdot (4.001 -$

155 $2)/4.001$, the values of $shape_t$ and $rate_t$ were then chosen in such a way that the mean of the

156 Gamma prior distribution was $E[S_t^2]$ and its variance $\left(\frac{E[S_t^2]}{3}\right)^2$.

157

158 *2.2 Metropolis-within-Gibbs sampling algorithm*

159   A 'Metropolis-Hastings within Gibbs' algorithm was implemented to sample from the

160 posterior distribution of all parameters (Gelman et al., 2004; see Wallach et al., (2012) for an

161 application to estimating crop growth model parameters). Briefly, the Gibbs sampler (Gelman et

162 al., 2004) is a Markov chain algorithm for high-dimensional parameter spaces. Because the

163 algorithm samples parameters sequentially from the conditional (on the data and all other

164 parameters) posterior distribution of each, the algorithm is highly efficient. With the exception of

165 T_{ti}, the conditional posterior distributions of all parameters in CGM-WGP are recognizable

166 distributions that can be sampled from directly. A Metropolis-Hastings step, which is an accept-

167 reject algorithm that can sample from any distribution, was therefore included in the final

168 algorithm to sample T_{ti}. The Gibbs sampler use in this study is identical to the Gibbs algorithm

169 generally used for BayesA models (Meuwissen et al., 2001; Yang and Tempelman, 2012), except

170 for the sampling of T_{ti} with the Metropolis-Hastings algorithm.

171   Conditional on the marker effects u_{tk}, the physiological traits T_{ti} of one individual are

172 independent of those of the others and can hence be sampled sequentially. The different traits for

173 each individual, however, are not and have to be sampled jointly. This was done as described by

174 Wallach et al. (2012), with the exception that a change of variable was implemented to sample the

175 parameters in the space of the natural logarithm. This is a common technique when the parameter

176   values in the original space have to be positive (Gelman et al., 2004). The Metropolis-Hastings

177   step was run for two subsequent iterations to improve convergence.

178   Gibbs sampling chains were run for 200 thousand iterations. The first half of each chain

179   was discarded as 'burn-in' and samples from every 100th iteration thereafter were stored, thus

180   resulting in 1000 stored samples. Convergence was monitored by inspecting graphical

181   diagnostics such as implemented in the R package 'coda' (Plummer et al., 2006). Increasing the

182   chain length did not seem to improve prediction accuracy. The algorithm was implemented as a C

183   routine and embedded in the R statistical software environment (R Core Team, 2014).

184

185   *2.3 Prediction of yield from CGM-WGP results*

186   The predicted yield of an untested individual i' in environment j' was obtained from the

187   posterior samples of the marker effects u_{tk} and the intercepts β_{o_t}. From each posterior sample the

188   values of the physiological traits were calculated as $\tilde{T}_{ti} = \beta_{o_t} + \sum_k z_{tik} u_{tk}$. Those values were

189   then entered into the CGM together with the inputs of the environment, resulting in one simulated

190   yield value per posterior sample. Those samples represent the posterior predictive distribution of

191   yield for individual i' in environment j'. The mean of this distribution was used as the predicted

192   value. The algorithm BayesA (Meuwissen et al., 2001) was utilized as a reference method that

193   predicts yield using marker information only. i.e., $\bar{y}_{i.} \sim N(\beta_o + \sum_k z_{ik} u_k , \sigma_e^2)$, with $\bar{y}_{i.}$ denoting

194   the yield of individual i averaged over all environments considered for estimation. The prior of

195   the marker effects u_k was $u_k \sim N(0, \sigma_k^2)$ and standard, uninformative prior distributions were

196   used for σ_k^2 and σ_e^2. The BayesA Gibbs-sampler was run for 50000 iterations, of which the first

197   25000 were discarded and samples from only every 25th subsequent iteration stored. In this study,

198   BayesA served as a purely statistical reference method relative to which we measure the benefit

199   of modeling G×E interactions with CGM-WGP.

200

201 *2.4 Crop growth model*

202 The CGM connected to the WGP algorithm is a mechanistic model based on the concept

203 of radiation and water capture and use efficiencies, and mass allocation to reproductive growth

204 (Muchow et al., 1990; Muchow and Sinclair, 1991). Crop and canopy development are simulated

205 as a function of thermal time (TT, °C) with base temperature for preflowering equal to 8°C and

206 postflowering equal to 0°C (Muchow et al., 1990). Growth (W) is calculated as the product of

207 light interception (LI) and radiation use efficiency (RUE), W=LI × RUE. The value for RUE was

208 set to 1.85 g MJ^{-1} after Hammer et al. (2009), unless explicitly changed for specific studies

209 described below. Light interception is estimated from the leaf area per plant (LP), plant density

210 (PD) and canopy attributes described by the coefficient of extinction, which has set to 0.4, LI=1-

211 exp(-0.4 × LP × PD). Leaf area per plant is modeled solely as a function of the size of the largest

212 leaf (AMAX, Birch et al., 1998); that is, other parameters are kept constant as in Muchow et al.

213 (1990). Transpiration (TR) is calculated as a function of W, vapor pressure deficit (VPD),

214 transpiration efficiency coefficient (TE=9 kPa, Tanner and Sinclair, 1983), and the expression of

215 the limited transpiration trait (Sinclair et al., 2005; Messina et al., 2015) on an hourly (h) time

216 step,

217
$$TR_h = \frac{W_h \times BKP}{TE} + \frac{W_h \times (VPD_h - BKP) \times SF}{TE} \quad \text{if } VPD \geq BKP$$

$$TR_h = \frac{W_h \times VPD_h}{TE} \quad \text{otherwise}$$

218 where BKP is the breakpoint and SF is the sensitivity of TR to VPD. The parameter SF was set at

219 0.3 in order to incorporate relevant functional biological behavior (Gholipoor et al., 2013;

220 Choudhary et al., 2014; Shekoofa et al., 2015). When hourly VPD exceeds BKP, hourly growth

221 W_h is updated to conform to hourly TR and a constant TE,

222 $$W_h = \frac{TR_h \times TE}{VPD_h}$$

223   Water deficit effect on growth is modeled through the coefficient water supply-to-

224 demand (SD) ratio. Water demand is calculated as TR in the absence of soil water deficit. Water

225 supply is estimated as the sum across all soil layers of soil water content minus the soil water

226 content at the lower limit times the *kl* as in Robertson et al. (1993), where the *kl* coefficient was

227 set at 0.08 (Dardanelli et al., 1997; Hammer et al., 2009). Soil water content is estimated using a

228 multilayer model. Grain yield is simulated as the linear increase of harvest index (HI) during seed

229 fill. Reduction in postflowering growth due to stress at flowering time is simulated by modeling

230 the attainable HI from silk numbers exerted at the onset of the increase in HI, as defined in

231 Muchow and Sinclair (1990), and the maximum silk numbers (SNM), a value that can vary

232 among genotypes. Silk number (SN) is estimated from the ear mass (EM) as, SN = SNM × (1 −

233 exp(-0.14 × (EM − MEB)), where MEB is a parameter characteristic of genotype (Cooper et al.,

234 2014), and EM is modeled using an exponential function of TT and a stress factor directly

235 proportional to SD. The parameter MEB corresponds to the threshold of ear biomass below which

236 silk elongation is not fast enough to exert silks beyond the ear husk. Chenu et al. (2009) used a

237 similar approximation that included a threshold similar to MEB to model the connection between

238 QTL controlling silk elongation, anthesis-silking interval, which is a crop attribute closely related

239 to yield under water limited conditions (Bolaños and Edmeades, 1993; Cooper et al., 2014), and

240 yield. For further discussion of CGMs Soltani and Sinclair (2012) provide an extensive treatment

241 of simple mechanistic crop models.

242

243 *2.5 Multi-environment trial simulation*

244   A multi-environment trial simulation experiment based on three environments was

245 created to assess the CGM-WGP methodology. To characterize the three environments and

246   quantify water availability during the crop cycle, water SD ratios were calculated on a daily time

247   step following the procedures described by Cooper et al. (2016). Consequently it was determined

248   that the simulated multi-environment trial comprised of three environments with different degrees

249   of water deficit occurring in Johnston, Iowa, US (41.684 °N, -93.508°W) in 1988, 2012 and

250   2010, herein referred to as water limited 1 (WL1), water limited 2 (WL2) and NWL (not water

251   limited), respectively. The soil depth, soil water holding capacity, and *kl* were 2.2 m, 0.13

252    $cm^3.cm^{-3}$, and 0.08, respectively. Planting dates were 4/29/1988, 4/28/2010, and 5/4/2012. Plant

253   population was set at 6.5 pl m^{-2}. Daily meteorological records were from the National Oceanic

254   and Atmospheric Administration (NOAA; Bell et al., 2013). Genotypic variation for a set of

255   physiological traits was considered for a Doubled Haploid (DH) population of lines. The DH

256   lines were evaluated as F1 hybrids in combination with an inbred from a complementary heterotic

257   group. Parameters describing these traits for an individual DH within a population were allowed

258   to vary within the following intervals: [700 < AMAX< 1100 cm^2] (Elings, 2000), [1.6 < RUE<2.1

259   g MJ^{-1}] (Sinclair and Muchow, 1999), [0.5<MEB<1.0 g] (Cooper et al., 2014), and

260   [1.5<BKP<2.5 kPa] (Messina et al., 2015).

261   The DH genotypes of the DH lines were generated *in silico* in two step process, similar to

262   the one used by Technow et al. (2014a) for simulating a DH maize breeding population. In step

263   one, an ancestral population of 50 inbred lines was stochastically simulated. The genome

264   consisted of 10 chromosomes with lengths between 0.75 and 1.25 Morgan (M). Two hundred

265   evenly spaced biallelic marker loci were placed on each chromosome. The total number of

266   markers was thus 2000. An additional 40 loci were randomly distributed across all chromosomes

267   that served the purpose of simulating quantitative trait loci (QTL). Historical linkage

268   disequilibrium (LD) between markers as well as their allele frequencies was simulated with the

269   method described by Montana (2005). The simulated expected LD (measured as squared

270   correlation) between markers followed an exponential decay, such that it halved approximately

271 every 0.1 Morgan. For two marker loci t Morgan apart, the expected LD followed $0.5 \cdot$

272 $2^{(-t/0.1)} + 0.1 \cdot 2^{(-t/0.5)}$. Exponential decay curves mirror the LD decay curves observed in

273 maize (Technow et al., 2014b). Minor allele frequencies were drawn at random from the $(0, 0.5)$

274 interval. This population was then random mated for three generations to generate a pedigree and

275 sub-population structure. The population size was thereby kept constant at 50. After the last

276 generation 1000 doubled haploid lines were generated through meiosis followed by a

277 chromosome doubling step.

278 The values for the physiological traits were simulated according to Technow et al.

279 (2015). A unique set of ten of the 40 loci set aside as QTL were assigned to each of the four

280 physiological traits: AMAX, RUE, MEB, and BKP. The additive substitution effect of each QTL

281 was drawn from a Standard Normal distribution and raw genetic scores calculated for each trait

282 by summing the effect of the QTL according to the genotypes of the DH lines. These scores were

283 then rescaled linearly to the ranges described above.

284 The true grain yield value of a DH line i in environment j was then simulated by

285 executing the CGM with the physiological trait values of the DH and the appropriate

286 environmental inputs. For those DH that became part of the estimation set we also simulated

287 observed phenotypic yield values by adding a Normal noise variable to the true values. The

288 variance of this variable was chosen in such a way that the within environment heritability was

289 equal to 0.66.

290 *2.6 Whole genome prediction application*

291 Estimation sets for training the CGM-WGP model were constructed from one, two or all

292 three environments. For the single location estimation sets (WL1, WL2 or NWL) the phenotypic

293 yield data of a random sample of 500 of the DH lines in that environment were used. For two and

294   three environment estimation sets, yield data from 250 DH lines in the two environments case and

295   166 DH lines in the three environments case were used. The total number of data points was thus

296   equal in all cases. Values for $\hat{m}_t$ and $\hat{v}_t$, which are required for calculation of constants and

297   starting values, were computed from estimates obtained from a random sample of 25 DH lines,

298   which were assumed to be phenotyped for the traits but were not used as part of the estimation

299   set. The CGM-WGP algorithm was then run as described and the marker effects used to predict

300   the yield performance of all DH lines within the validation set in all three environments, also as

301   described. Prediction accuracy was then calculated as the Pearson correlation between predicted

302   and true yield in each environment. Because the true values of the physiological traits were

303   known, it was possible to assess their prediction accuracy by calculating the correlation between

304   their predicted and true values. BayesA methodology was utilized as a reference method and it is

305   described above. The whole process, including the data simulation, was repeated 75 times for

306   each environment combination. The resulting distribution of the accuracy statistics was

307   summarized by the mean and standard deviation.

308

309   *2.7 Empirical breeding experiment*

310   For the empirical evaluation the CGM-WGP and BayesA methods prediction accuracies

311   were compared using four DH populations that were tested in an experiment that comprised of a

312   non-water-limited (NWL) environment and a water-limited (WL) environment. Both field

313   environments were created at the DuPont Pioneer Viluco research station, which is located in

314   Chile (-33.797 °S, -70.807 °W), in the 2012/13 season. The contrasting water environments were

315   created by controlled application of quantity and timing of water during the crop cycle. As for the

316   simulation experiment, water SD ratios were estimated on a daily time step during the crop cycle

317   for the NWL and WL environments to quantify the impact of the different irrigation regimes that

318   were used to create the contrasting water environments.

319   The four DH populations, referred to as DHPop1, DHPop2, DHPop3, DHPop4, were

320   created from biparental crosses between six inbred lines, referred to as I1, I2, … , I6. The two

321   parents of DHPop1, I1 and I2, were different from the four inbred lines, I3, I4, I5 and I6, used as

322   parents to create the other three DH populations. One of the four remaining inbred lines, I3, was

323   used as a common parent for all three remaining DH populations; DHPop2 parents I3/I4,

324   DHPop3 parents I3/I5 and DHPop4 parents I3/I6. Thus, there is a closer pedigree relationship,

325   based on the half-sib structure, between DHPop2, DHPop3 and DHPop4 than there is between

326   any of these three populations and DHPop1. Each of the four populations was represented in the

327   experiment by 76 to 105 DH lines. The DH lines were each genotyped with approximately 1600

328   polymorphic Single Nucleotide Polymorphism (SNP) markers.

329   For the experimental evaluation of grain yield, testcross hybrids were created for all of

330   the DH lines using a common inbred tester line that was selected from a complementary heterotic

331   group. Thus, while for discussion purposes we refer to DH lines they were evaluated for grain

332   yield as hybrids in the NWL and WL environments. Grain yield was measured for all DH lines

333   from two-row plots. The two-row plots were 4.5m long with 0.75m spacing between rows. The

334   number of plants within the rows was managed to represent a plant population of 7.9 pl. m^{-2}. To

335   manage irrigation quantity and timing drip tape was installed at a depth of approximately 0.1m

336   and approximately 0.1m to the side of each plot row at the time of planting of the experiment. At

337   maturity the total grain yield of a plot was measured by harvesting all ears from within the plot

338   using a two-plot combine harvester. The total weight and moisture content of the grain from a

339   plot were measured at the time of harvest and the harvested plot weight was converted to grain

340   yield on an area basis at 15% moisture.

341   The experimental design in each environment was a row-column design with two

342   replicates. The grain yield data were analyzed using the ASREML mixed model software

343   (Gilmour et al. 2009). For the mixed model analysis the two environments, NWL and WL, were

344   treated as fixed effects and the DH lines were treated as a random sample of lines from within

345   their respective population. To investigate the magnitude of G×E interaction for grain yield

346   between the NWL and WL environments for each of the four DH populations a combined

347   analysis of variance was conducted following the recommendations of van Eeuwijk et al. (2001).

348   When significant G×E interactions were detected the genetic correlation was estimated for grain

349   yield between the two environments (Falconer and Mackay 1996). For reference, the genetic

350   correlation can range from 1.0 to -1.0. A genetic correlation of 1.0 indicates there were no G×E

351   interactions. Conversely, a genetic correlation of -1.0 indicates strong G×E interactions with

352   complete rank reversal of the DH lines between the two environments. For the selected mixed

353   model analysis of variance Best Linear Unbiased Predictors (BLUPs) were computed for grain

354   yield of each of the DH lines in the NWL and WL environments. These grain yield BLUPs were

355   then used for the CGM-WGP and BayesA prediction analyses.

356   A leave-one-family-out cross-validation was conducted to assess prediction accuracy for

357   grain yield. Here the CGM-WGP model was selected using an estimation data set based on the

358   yield data from both the NWL and WL environments for three of the four DH populations and

359   then used to predict the yield values of the fourth DH population for both the NWL and WL

360   environments. This process was repeated until each population was left out once. Since the

361   estimation set comprised yield data from both the yield in the NWL and WL environments this is

362   a multi-environment estimation set. Prediction accuracy for the lines of the DH population left

363   out of the estimation set was calculated as the correlation between predicted and observed yield

364   BLUP values separately for both the NWL and WL environments.

365   The physiological traits for the empirical study were the same as those used for the

366   simulation study; AMAX, RUE, MEB and BKP. Prior estimates of physiological trait means and

367   variances ($\hat{m}_t$ and $\hat{v}_t$) covered the typically observed biological ranges. The values of the means

368   were $\hat{m}_{AMAX} = 850$, $\hat{m}_{RUE} = 1.85$, $\hat{m}_{BKP} = 2.0$, and $\hat{m}_{MEB} = 0.75$ and those of the variances

369    $\hat{v}_{AMAX} = 76.5^2$, $\hat{v}_{RUE} = 0.13^2$, $\hat{v}_{BKP} = 0.25^2$, and $\hat{v}_{MEB} = 0.13^2$. The values of $\hat{v}_{e_j}$ were

370    $\hat{v}_{e_{FS}} = 144.0^2$ and $\hat{v}_{e_{WW}} = 70.3^2$. Both of which were obtained from an ASREML analysis of

371   the original data.

372   The classical BayesA WGP model (Meuwissen et al. 2001) was used as a reference

373   method relative to which we measure the benefit of modeling G×E interactions with CGM-WGP.

374   The BayesA model was applied directly to the BLUP yield average over the two environments.

375

376   *2.8 Large scale evaluation of hybrids never tested in the field*

377   The CGM-WGP methodology can be used to make predictions within the set of

378   experiments used for model training and evaluation, as demonstrated by Cooper et al. (2016).

379   This application is comparable with BayesA and other statistical based methodologies (Heffner et

380   al. 2009, Lorenz et al., 2011). Because CGM-WGP estimates the value of the alleles for each

381   polymorphic marker locus for each physiological parameter included for CGM-WGP model

382   training, it is possible to generate predictions for any combination of management and

383   environment for any individual that has been genotyped and belongs to the genetic inference

384   space. A simulation experiment using genetic parameters estimated for individuals from a

385   breeding population (see above) and environments included in the TPE (Messina et al., 2015) was

386   conducted to demonstrate the feasibility of augmenting field evaluation with in-silico evaluation

387   of untested genotypes at large scale. Parameters to run the mechanistic CGM model were

388   estimated for individuals from a breeding population using the method and breeding experiments

389   described above. Environment and management inputs to run the CGM in 2263 30 x 30 km grids

390   within the maize growing region for 1988 and 2014 are described in Messina et al. (2015).

391   Briefly, weather data were from NOAA. Solar radiation was estimated from temperature records

392   (Bristow and Campbell, 1984) with parameters provided by Mud Springs Geographers, Inc, and

393   hourly vapor pressure deficit (VPD) was estimated from daily temperature assuming an harmonic

394   change in daily cycle (Monteith and Unsworth, 1990). Soil depth was from the STATSGO

395   database (United States Department of Agriculture, 2015) and used to estimate total soil water

396   holding capacity by multiplying it by a constant (0.13 cm^{-3} cm^{-3}) volumetric fraction of available

397   soil water. Crop management data that includes plant population, planting date and maturity

398   group were from DuPont Pioneer data bases.

399

3. Results and Discussion

3.1 Physiological determinants of G×E interactions for yield

402   The simulation study included three environments contrasting for water availability, as

403   characterized by the water supply to demand ratio index (Fig. 2). Water deficit was largest at

404   flowering time in WL1 and at grain filling in WL2. Simulations for the year 2010 (NWL)

405   indicated absence of water stress with SD equal to 1 throughout the growing season (SD for NWL

406   not shown on Fig. 2). This combination of environments set the conditions to observe differential

407   effects of physiological traits on yield (Fig. 3) and consequently create a case study to test the

408   CGM-WGP and BayesA algorithms for ability to construct predictive genetic models (Tables 1,

409   2).

410   Figure 3 shows the conditional influence of the four physiological traits on yield in the

411   three environments when holding the other traits constant at their mean and yield is standardized

412   relative to the distribution when all traits are varying. Because of the occurrence of stress around

413   flowering time (Fig. 2), MEB has the largest impact on yield in environment WL1 (Fig. 3b).

414   Yield and drought tolerance in maize decreased in WL1 with increasing MEB, as demonstrated in

415   previous studies (Messina et al., 2011, Cooper et al. 2014). With increasing AMAX (Fig. 3a),

416   RUE (Fig. 3c) and BKP (Fig. 3d) traits yield increased in the NWL environment and decreased in

417   the drought stress environments WL1 and WL2. These results are consistent with those observed

418   in other studies (Sinclair and Muchow, 2001; Messina et al., 2011; Messina et al., 2015). The

419   traits AMAX, RUE and BKP regulate crop canopy level transpiration thus the water use

420   dynamics during the growing season. Water use decreases with decreasing values of any of these

421   traits, which is a mechanism to conserve water during the vegetative period. When water deficit

422   occurs at flowering time, water conservation may have a large impact on yield (Cooper et al.

423   2014a). Because of the high sensitivity of silking to water deficit (Hall et al., 1982; Bolaños and

424   Edmeades, 1993), the greater intensity of water deficit at flowering time in WL1 (Fig. 2) yield in

425   WL1 decreased with increasing AMAX, RUE and BKP traits more than in WL2 (Fig. 3). At a

426   constant value of AMAX, RUE, BKP or MEB, simulated yield using the CGM can increase,

427   decrease or show no change depending on the environment. This G×E interaction for yield,

428   resulting from the interplay between physiological process and the environment, was previously

429   referred as functional emergent behavior (Hammer et al., 2006). This attribute of the CGM to

430   generate variable outputs conditional to a vector of constants that characterize physiological traits

431   is what make these algorithms potentially useful functions to construct simple additive predictive

432   genetic models for traits incorporated into the CGM that can produce complex outputs that

433   reproduce G×E interactions and fitness landscapes for yield (Messina et al., 2011; Hammer et al.,

434   2006; Hammer et al., 2010).

435

3.2 CGM-WGP incorporates biological insight within genomic prediction algorithms and

increase prediction accuracy

The simulation results reported in this study introduce enhanced realism relative to Technow et al. (2015) with yield responses to physiological trait variation more subtle and linear than in the previous study (Fig. 3). The average prediction accuracy of CGM-WGP when trained in one, two or three environments was 0.55 (Table 1), 0.75 and 0.75 (Table 2), respectively. In contrast, the average prediction accuracy for BayesA was 0.24 for one (Table 1), 0.23 for two and 0.32 for three (Table 2) training environments, respectively. Despite the absence of major non-linear yield response to variation in physiological traits, as in Technow et al. (2015), the results from this study support the conclusion that CGM-WGP increased prediction accuracy over the BayesA method by incorporating biological insight into the prediction algorithm.

Although the CGM-WGP average accuracy was greater than for BayesA, there were cases where BayesA accuracy could be equal or greater than CGM-WGP's (Table 1), for example, when the prediction and the estimation environments were alike due to the common effects of drought (WL1, WL2). Cooper et al. (2016) reported similar results for an application of CGM-WGP to two drought environments that were part of a MET from within a breeding program. In contrast, there were no cases where the accuracy of BayesA was greater than that for CGM-WGP when the estimation environment differed from the prediction environment (e.g., WL1 vs. NWL). In the presence of the emergent G×E interactions at the yield level due to the contrasting influences of the physiological traits in the different environments (Fig. 3) BayesA accuracy could be negative (Table 1). For example, when BayesA was trained in WL1 and predictions were made in NWL, the mean prediction accuracy was -0.62. As should be expected similar results were obtained for the reverse scenario when BayesA was trained in NWL and

459   predictions were made in WL1 (r= -0.60, Table 1). Negative prediction accuracies were not

460   observed for CGM-WGP ($r \geq 0.22$, Table 1), indicating the algorithm was able to define genetic

461   models for physiological adaptive traits that account for the presence of G×E interactions and the

462   effect of the variable environments on the prediction of yield performance.

463   Prediction accuracy for both CGM-WGP and BayesA increased with increasing number

464   of estimation environments (Table 1, Table 2). The pattern observed for estimation and prediction

465   using single environment data remains evident when more than one environment is included in

466   the estimation set (Table 2). Negative prediction accuracy was still estimated for BayesA when

467   estimation and prediction environments were dissimilar but not for CGM-WGP (Table 2).

468

469   *3.3 Prediction accuracy depends on environment type that reveals genetic variation in adaptive*

470   *physiological traits*

471   Prediction accuracy for physiological traits depends on the environment type of the

472   estimation set (Table 3). While highest accuracies for BKP were estimated when estimation sets

473   were drought environments WL1 and WL2, highest accuracy for AMAX and RUE were

474   estimated when the estimation set was NWL environment (Table 3). Yield increased markedly

475   with increasing AMAX and RUE within the NWL environment (Fig. 3), which is associated with

476   the highest accuracy attained for these two traits in this environment type. Because the magnitude

477   of the yield response to change in MEB depends on intensity of water deficit at flowering time

478   (Fig. 3, Fig. 2), the highest accuracy for the estimation of MEB was observed when data from

479   WL1, which experienced the greatest level of water deficit at flowering, was used as the

480   estimation set (Fig. 2; Table 3). With the absence of (NWL) or moderate (WL2) water deficit at

481   flowering time, low prediction accuracy was estimated for MEB when these environments were

482   used as estimation sets, -0.03 and 0.17, respectively. These differential accuracies for estimating

483   physiological traits translate into variable accuracies for yield prediction. While accuracy of yield

484   prediction for environment WL2 using a model trained using data for WL1 is 0.51, the accuracy

485   for the reciprocal is 0.34 (Table 2). Similarly, the accuracy of prediction in WL1 using a model

486   trained using data from WL2 and NWL is 0.72, which is lower than for other combinations (0.79

487   and 0.76). Overall accuracy for yield and physiological trait prediction increased with increasing

488   number of environments included in the estimation set (Tables 1, 2, 3, 4) as more environment

489   types are included that expose variation in adaptive physiological traits enabling the algorithm to

490   find adequate genetic models. This new evidence suggests that further improvements in

491   predictability may be possible by leveraging managed stress environments and optimizing the

492   combinations of types of environments required to expose genetic variation for adaptive traits.

493

494   *3.4 CGM-WGP improved prediction accuracy relative to BayesA for systems where G×E is an*

495   *important determinant of yield is demonstrated in breeding trials*

496   As in the simulation study above, for the empirical study prior to analysis of the grain

497   yield data and application of the CGM-WGP and BayesA methods the impact of the different

498   irrigation management strategies was investigated to characterize the two environments.

499   Following the same procedures described above for the simulation study, the daily time step

500   water SD profiles were determined for the Viluco well-watered and water-limited irrigation

501   treatments (Fig. 4). For the well-watered treatment the SD profile remained at, or close to, 1.0 for

502   the duration of the crop cycle. Thus, the well-watered treatment was managed to realize a non-

503   water-limited environment (NWL). For the water-limited treatment irrigation was reduced,

504   commencing in the vegetative stage around V7, and the SD profile decreased to a value below

505   0.2, coinciding with the timing of flowering for the DH populations tested. After flowering of the

506   DH families was completed irrigation was resumed and the SD profile increased and was

507 maintained between 0.5 and 1.0 for the remainder of the crop cycle. Thus, the water-limited

508 treatment was managed to realize a water-limited environment (WL), where the peak of the water

509 limitation was imposed during flowering time of the DH lines to impact yield development

510 through imposition of a flowering stress drought. Therefore, the testing of the four DH

511 populations in the combination of the NWL and WL environments provided a suitable empirical

512 MET for evaluating the CGM-WGP methodology, where the traits of interest were relevant for

513 predicting grain yield of the maize DH lines in drought and non-drought environments, as was

514 demonstrated in the simulation study.

515   Analysis of variance indicated that there were significant G×E interactions for grain yield

516 between the NWL and WL environments for all four DH populations. Therefore, further analyses

517 of variance for each DH population focused on the genetic correlation for yield between the two

518 environments and the magnitude of genetic variance for yield within the NWL and the WL

519 environments (Table 5). There was significant genetic variation for grain yield in the NWL and

520 WL environments for all four DH populations. The magnitude of the variance components for

521 yield in the WL environment was greater for DHPop3 and DHPop4 compared to DHPop1 and

522 DHPop2 (Table 5). For the NWL environment, the magnitude of genetic variance for yield was

523 greater for DHPop4 than for the other three DH populations. The genetic correlation for grain

524 yield between the NWL and WL environments differed among the four DH populations (Table

525 5). To visualize the different magnitudes of genetic variance for grain yield and the different

526 genetic correlations between the NWL and WL environments scatter diagrams were constructed

527 for each DH population for the grain yield BLUPs (Fig. 5). For DHPop1 (Table 5, Fig. 5a) there

528 was no correlation between NWL and WL. For DHPop2 there was an indication of a negative

529 genetic correlation (Table 5, Fig. 5b). For both DHPop3 (Table 5, Fig. 5c) and DHPop4 (Table 5,

530 Fig. 5d) there was a positive correlation. The different grain yield results for the four DH

531 populations provides evidence that the physiological and therefore the genetic basis of the grain

532 yield variation expressed in the NWL and WL environments differed among the four DH

533   populations. Therefore, the results obtained from the empirical MET encompass a number of the

534   scenarios examined in the simulation study and represent important technical issues that need to

535   be addressed in an applied maize breeding program.

536   On average CGM-WGP ($r = 0.34$) resulted in higher prediction accuracy than BayesA (r

537    $= 0.23$) over all predication scenarios considered for the four DH populations (Table 6). Both

538   CGM-WGP and BayesA had higher prediction accuracy for the WL environment ($r = 0.45$ and

539   0.33, respectively) than for the NWL environment ($r = 0.23$ and 0.14, respectively). In the WL

540   environment the prediction accuracy was positive for all DH populations for both CGM-WGP

541   and BayesA (Table 6). Further for all four DH populations the prediction accuracy for the CGM-

542   WGP was higher than for BayesA for the WL environment. For the NWL environment CGM-

543   WGP achieved positive prediction accuracy for all four DH populations. However, for BayesA

544   the ability to achieve a positive prediction accuracy for the NWL environment depended on the

545   DH population. For two of the DH populations (DHPop1 and DHPop3) positive prediction

546   accuracy was achieved, while for the other two DH populations (DHPop2 and DHPop4) it was

547   not possible to predict grain yield in the NWL environment. Collectively the prediction accuracy

548   results indicate that compared to the BayesA methodology, which was applied to the average

549   grain yield performance across the WL and NWL environments, there were realized advantages

550   in prediction accuracy for yield in both the WL and the NWL environments from the modeling of

551   the G×E interactions between the WL and NWL environments by the CGM-WGP methodology.

552

553   *3.5 Evaluation of germplasm in virtual environments augments empirical testing through*

554   *simulation of untested hybrids in large scale evaluation trials*

555   In this paper a set of yield predictions were made to compare CGM-WGP methodology

556   with BayesA using a breeding population (Table 6). Because yield predictions were made

557 utilizing the CGM-WGP methodology, parameters to run the mechanistic CGM could be

558 estimated for these lines from genotypic information and allele values. Figure 6a shows simulated

559 yields for two DH lines in 2263 grids in 2014 and 1988. Yield for DH line 1 showed higher yields

560 than DH line 2 virtually across the U.S. corn belt in 2014 but not in 1988. The yield differential

561 varied with geography indicating G×E interactions. Indeed, the relationship between DH line 1(x)

562 and 2 (y) across all grids and the two years characterized using a linear regression model is

563 $y = 51.8(\mp0.6) + 0.94(\mp0.00051)x$. From these parameters it is feasible to estimate that DH

564 line 1 perform better than DH line 2 in environments where yield is greater than 877 g m^{-2} but not

565 below this threshold. Further evaluations were conducted for two years and 34 DH lines (Fig. 6).

566 This level of testing is not feasible using empirical approaches even at advanced stages of product

567 evaluation, but views of plausible performance that can inform testing could become available for

568 untested DH lines. These results demonstrate reduction to practice of the methodology at the

569 scale of the early hybrid advancement stages of a breeding program. The method demonstrated in

570 this paper enable simulation studies that inform decision about the creation of products and their

571 plausible placement in different geographies and cropping systems.

572

573 **4. Implication for crop model development and application**

574   The integration of the hierarchical model with the Metropolis-Hastings within Gibbs

575 algorithm enabled using multiple sources of data, observed and virtual, to evaluate CGM-WGP

576 prediction skill. This method is a significant advancement relative to and advocated by prior

577 studies (Technow et al., 2015; Cooper et al., 2016). This enhanced capability enabled studies that

578 demonstrated that increasing the number of environments per se does not necessarily increase

579 predictive accuracy of CGM-WGP but the combination of environment types that enable

580 expression of relevant genetic variation for adaptive physiological traits is a productive approach

581 to increase predictive accuracy.

582   To realize potentially higher predictive skills, CGMs must incorporate quantitative

583   biological relations that can capture the expression of traits when these are exposed as a result of

584   new experimental designs and precision phenotyping. Many of these relations are unknown and

585   likely surface to the known with the creation of new germplasm and genetic diversity. While the

586   construction of the CGM used in this study was guided by prior research on relevant traits

587   influencing yield in WL and NWL environments (Hammer et al., 2009; Messina et al, 2009;

588   Messina et al., 2011; Choudhary et al., 2014; Cooper et al., 2014 ; Messina et al., 2015; Reyes et

589   al., 2015; Cooper et al., 2016) it was possible to identify variation in predictive accuracy among

590   breeding populations and examples where CGM-WGP was not better than the reference BayesA

591   method. More cases such as this should be expected and suggest the need to consider plausible

592   avenues of research and development to maximize the opportunities to realize improved

593   accuracy. Out of many plausible solutions the development of a "second generation crop growth

594   model" (SCGM) and the link between Phenomics and CGM are considered briefly.

595   A SCGM for use within CGM-WGP is designed and created within a dynamic

596   framework that enables rapid changes in the CGM to align it to evolving WGP algorithms,

597   germplasm, breeders' questions and objectives, to leverage phenomics capabilities, and to

598   effectively deal with scientist bias. Brown et al. (2014) demonstrates a promising framework to

599   enable the development of models of various complexities and that could be evolved quickly by

600   practitioners. A missing component to Brown's framework is a life cycle management system

601   that provides guidance to the needs of creating new models as well as to retire models. The

602   implementation of authoritative repositories of quality experimental data is necessary to a SCGM

603   life management system and eliminates the need for centralized controlled systems that may

604   delay the implementation of SCGM. Holsworth et al. (2014) discuss promising opportunities

605   such as "The Stack" that can enable model evaluation but also simulation at global scale,

606   extending the application demonstrated in this research for the U.S. corrn belt to other crops and

607   geographies.

608   A SCGM will be applied to experiments with increasing size, data type diversity

609   generated by phenotyping platforms, and complexity. Although the metropolis-within Gibbs

610   sampling algorithm introduced here can improve the efficiency and decrease computing demands,

611   as demonstrated in this paper, it is inevitable that faster models will be required to work with

612   larger and more complex breeding experiments, involving hundreds of environments and

613   thousands of genotypes from diverse germplasm sources, where convergence due to a more

614   complex system may require increasing the number of iterations to reach convergence. Runtime

615   will become even more relevant as stochasticity is incorporated into SCGM to deal formally with

616   measurement error, environmental uncertainty, and internal stochasticity characteristic of

617   complex systems (Wallach et al., 2012; Technow et al., 2015). Such models in combination with

618   faster algorithms will enable answering fundamental questions about the role of internal system

619   variability on the determination of predictability. Both the need to explore larger CGM parameter

620   spaces when applying the model to new breeding populations, and the availability of trait

621   information that will force identification of solutions that satisfy multiple constraints suggests that

622   a fundamental area of research can focus on how predictability and prediction skill changes with

623   CGM-WGP complexity. As model complexity increases, so will the unknowns and the

624   complexity of the performance landscape that may reduce the ability to find global optima.

625   Answers to these questions will enable designing improved strategies to effectively deal with

626   limited predictability to accelerate genetic gain.

627   Phenomics and SCGM will be integrated to form a virtuous cycle of mutual development

628   while delivering improved genetic and physiological mechanistic models, and improved

629   predictions (Cooper et al., 2002; Houle et al., 2010; Messina et al., 2011). High throughput

630   phenotyping platforms, here considered broadly to include managed stress environments, will

631   provide data to both train CGM-WGP and to enhance biological mechanistic models (Houle et

632   al., 2010; Cooper et al., 2014; Pauli et al., 2016). CGM can inform phenotyping based on known

633   physiological understanding but also serve as frameworks that help identify knowledge gaps

634   (Hammer et al., 2002). SCGM-WGP becomes the integration framework that enables the

635   incorporation of data for multiple traits, which are outputs from high throuhput phenotyping

636   platforms, genomic information, agronomy and environment. A model to enable such integration

637   could be of the form,

638
$$y_{ijp} \sim N\left(CGM\left(T_{ti}, E_j\right)_p, \sigma^2_{e_{jp}}\right)$$

639   where y_{ijp} is a set of measurable phenotypes (p) influenced by functional trait t and measurable

640   using platforms (eg. leaf area, leaf angle that influence functional traits, such as RUE, which are

641   captured in the relationships of the CGM) with error variance σ^2_e for phenotype p in environment

642   j. The methods described in this paper could be applied to train this model. This approach is a

643   significant change relative to the two stage approaches advocated to date (Xin et al, 2004;

644   Hammer et al., 2006; Chenu et al., 2009; Messina et al., 2011; Pauli et al., 2016) because it

645   provides an integrated and flexible framework to tune the utilization of phenomics to the breeding

646   or more general, to the plant science objective. Predictions from this model are testable

647   hypothesis with physiological and genetic components. It is less clear in the literature and a clear

648   area of future research how to extend the framework to handle knowledge gaps through

649   integration of polygenic terms that could be handled through statistical models within the

650   framework.

651

652   **5. Concluding remarks**

653   This research used a combination of simulation and empirical studies to explain how the

654   CGM-WGP methodology introduced by Technow et al. (2015) works to achieve enhanced levels

655   of prediction accuracy and to demonstrate reduction to practice for some applications to maize

656   breeding and product placement for target environments in the US corn-belt. This new

657   development in modeling, achieved through the integration of genetic and physiological modeling

658   capabilities, provides a research platform for enhancing predictions of crop yield that can account

659   for important components of G$\times$E$\times$M interactions that influence crop productivity. The

660   development of the hierarchical model enabled studies to demonstrate the critical use of diverse

661   environments as estimation sets for CGM-WGP as these reveal genetic variation for adaptive

662   physiological traits. Three important outcomes of the CGM-WGP methodology that merit further

663   consideration and investigation are: (1) The algorithm used within the CGM-WGP method to

664   connect genetic information to the traits that vary among genotypes and respond to environmental

665   conditions to influence yield is conducted as an integrated single step process. This single step

666   approach contrasts with previous two-step methods that first seek to identify genes or regions of

667   the genome (QTL) that map to traits proposed to influence yield, which are then in turn integrated

668   within the CGM as predictors in a second step. (2) Some of the requirements of high-throughput

669   phenotyping are relaxed and radically changed in comparison to the alternative two-step

670   approaches. In the two-step approaches advocated to date all individuals have to be phenotyped

671   for all traits in all environments to establish the relationship between genes or QTL and the traits

672   prior to integration into the CGM. For CGM-WGP this dense level of phenotyping may not

673   always be required, the phenotyping load can be reduced, and efforts seeking to generate large

674   volumes of data may be turned into efforts seeking to unravel the physiological basis of

675   adaptation and how to incorporate the resulting knowledge into mechanistic models. For many

676   applications emphasis can be placed on phenotyping efforts to establish the functional

677   relationships that are established within the CGM and to develop informative prior distributions

678   to be used with the CGM to enable the CGM-WGP. (3) New criteria are emerging as

679   foundational principles for developing a second generation of CGMs that explicitly incorporate

680   the concept of genetic variation for traits at different scales in biological hierarchies (e.g., cellular

681   to tissue to organ to crop canopy), and their functional relationships across these hierarchical

682   scales in biology.

683   **References**

684   Bell, J. E., M.A. Palecki, C.B. Baker, W.G. Collins, J.H. Lawrimore, R.D. Leeper, M.E. Hall, J.

685   Kochendorfer, T.P. Meyers, T. Wilson, and H. J. Diamond. 2013. U.S. Climate Reference

686   Network soil moisture and temperature observations. J. Hydrometeorol. 14:977-988.

687   Birch, C.J., Hammer, G.L., Rickert, K.G., 1998. Improved methods for predicting individual leaf

688   area and leaf senescence in maize (Zea mays). Aust. J. Agric. Res. 49: 249-262.

689   Bolaños, J., and G.O. Edmeades. 1993. Eight cycles of selection for drought tolerance in lowland

690   tropical maize. II. Responses in reproductive behavior. Field Crops Res. 31:253-268.

691   Bristow, K.L., and G.S. Campbell. 1984. On the relationship between incoming solar radiation

692   and daily maximum and minimum temperature. Agric. For. Meteorol. 31:159-166.

693   Brown, H. E., N.I. Huth, D.P. Holzworth, E.I. Teixeira, R.F. Zyskowski, J.N.G. Hargreaves, D.J.

694   Moot. 2014. Plant Modelling Framework: Software for building and running crop models on the

695   APSIM platform. Environmental Modelling & Software 62:385-398.

696   Chenu, K., S.C. Chapman, F. Tardieu, G. McLean, C. Welcker, and G.L. Hammer. 2009.

697   Simulating the yield impacts of organ-level quantitative trait loci associated with drought

698   response in maize: a "gene-to-phenotype" modeling approach. Genetics 183:1507-1523.

699   Choudhary, S., T.R. Sinclair, C.D. Messina, and M. Cooper. 2014. Hydraulic conductance of

700   maize hybrids differing in transpiration response to vapor pressure deficit. Crop Sci. 54:1147-

701   1152.

702   Cooper, M., S.C. Chapman, D.W. Podlich, and G.L. Hammer. 2002. The GP problem:

703   quantifying gene-to-phenotype relationships. In Silico Biol. 2:151-164.

704   Cooper, M., D.W. Podlich, and O.S. Smith. 2005. Gene-to-phenotype models and complex trait

705   genetics. Aust. J. Agric. Res. 56: 895-918.

706   Cooper, M., F.A. van Eeuwijk, G.L. Hammer, D.W. Podlich, and C. Messina. 2009. Modeling

707   QTL for complex traits: detection and context for plant breeding. Curr. Opin. Plant Biol. 12:231-

708   240.

709   Cooper, M., C.D. Messina, D. Podlich, L.R. Totir, A. Baumgarten, N.J. Hausmann, D. Wright,

710   and G. Graham. 2014. Predicting the future of plant breeding: complementing empirical

711   evaluation with genetic prediction. Crop Pasture Sci. 65: 311-336.

712   Cooper, M., F. Technow, C. Messina, C. Gho, and L. Radu Totir. 2016. Use of crop growth

713   models with whole-genome prediction: Application to a maize multienvironment trial. Crop Sci.

714   56:1-16.

715   Dardanelli, J.L., O.A. Bachmeier, R. Sereno, and R. Gil. 1997. Rooting depth and soil water

716   extraction patterns of different crops in a silty loam Haplustoll. Field Crops Res. 54:29–38.

717   Dong, Z., O. Danilevskaya, T. Abadie, C. Messina, N. Coles, and M. Cooper. 2012. A gene

718   regulatory network model for floral transition of the shoot apex in maize and its dynamic

719   modeling. PLoS ONE 7(8): e43450. doi:10.1371/journal.pone.0043450

720   Elings, A. 2000. Estimation of leaf area in tropical maize. Agron. J. 92: 436-444.

721   Fahlgren, N., M.A. Gehan, and I. Baxter. 2015. Lights, camera, action: high-throughput plant

722   phenotyping is ready for a close-up. Curr. Opin. Plant Biol. 24: 93-99.

723   Falconer, D.S. and T.F.C. Mackay. 1996. Introduction to Quantitative Genetics (Fourth Edition).

724   Longman Group Limited, Essex, England.

725 Furbank, R.T. and M. Tester. 2011. Phenomics — technologies to relieve the phenotyping

726 bottleneck. Trends Plant Sci. 16:635-644.

727 Gaffney, J., J. Schussler, C. Löffler, W. Cai, S. Paszkiewicz, C. Messina, J. Groeteke, J.

728 Keaschall, and M. Cooper. 2015. Industry-scale evaluation of maize hybrids selected for

729 increased yield in drought-stress conditions of the US corn belt. Crop Sci. 55: 1608-1618.

730 Gelman, A., J.B. Carlin, H.S. Stern, and D.B. Rubin. 2004. Bayesian data analysis. CRC Press,

731 Boca Raton, FL, USA.

732 Gholipoor, M., S. Choudhary, T.R. Sinclair, C.D. Messina, and M. Cooper. 2013. Transpiration

733 response of maize hybrids to atmospheric vapor pressure deficit. J. Agron. Crop Sci. 199: 155-

734 160.

735 Gilmour, A.R., B.J. Gogel, B.R. Cullis, and R. Thompson. 2009. ASReml User Guide Release

736 3.0 VSN International Ltd, Hemel Hempstead, HP1 1ES, UK.

737 Habier, D., R.L. Fernando, K. Kizilkaya, and D.J Garrick. 2011. Extension of the Bayesian

738 Alphabet for Genomic Selection. BMC Bioinformatics 12: 186.

739 Hall, A.J., F. Vilella, N. Trapani, and C. Chimenti. 1982. The effects of water stress and genotype

740 on the dynamics of pollen-shedding and silking in maize. Field Crops Res. 5:349-363.

741 Hammer, G.L., M.J. Kropff, T.R. Sinclair, J.R. Porter. 2002. Future contributions of crop

742 modelling—from heuristics and supporting decision making to understanding genetic regulation

743 and aiding crop improvement. Eur. J. Agron.18:15-31.

744 Hammer, G, M. Cooper, F. Tardieu, S. Welch, B. Walsh, F. van Eeuwijk, S. Chapman, and D.

745 Podlich. 2006. Models for navigating biological complexity in breeding improved crop plants.

746 Trends Plant Sci. 11:587-593.

747   Hammer, G.L., Z. Dong, G. McLean, A. Doherty, C. Messina, J. Schussler, C. Zinselmeier, S.

748   Paszkiewicz, and M. Cooper. 2009. Can changes in canopy and/or root system architecture

749   explain historical maize yield trends in the U.S. Corn Belt? Crop Sci. 49:299-312.

750   Hammer, G.L., E. van Oosterom, G. McLean, S.C. Chapman, I. Broad, P. Harland, and R.C.

751   Muchow. 2010. Adapting APSIM to model the physiology and genetics of complex adaptive

752   traits in field crops. J. Exp. Bot. 61:2185-2202.

753   Heffner, E.L., M.E. Sorrells, and J.-L. Jannink. 2009. Genomic selection for crop improvement.

754   Crop Sci. 49: 1-12.

755   Holzworth, D.P., N.I. Huth, P.G. deVoil, E.J. Zurcher, N.I. Herrmann, G. McLean, K. Chenu, E.J.

756   van Oosterom, V. Snow, C. Murphy, A.D. Moore, H. Brown, J.P.M. Whish, S. Verrall, J.

757   Fainges, L.W. Bell, A.S. Peake, P.L. Poulton, Z. Hochman, P.J. Thorburn, D.S. Gaydon, N.P.

758   Dalgliesh, D. Rodriguez, H. Cox, S. Chapman, A. Doherty, E. Teixeira, J. Sharp, R. Cichota, I.

759   Vogeler, F.Y. Li, E. Wang, G.L. Hammer, M.J. Robertson, J.P. Dimes, A.M. Whitbread, J. Hunt,

760   H. van Rees, T. McClelland, P.S. Carberry, J.N.G. Hargreaves, N. MacLeod, C. McDonald, J.

761   Harsdorf, S. Wedgwood, B.A. Keating. 2014. APSIM-Evolution towards a new generation of

762   agricultural systems simulation. Environmental Modelling & Software 62:327-350.

763   Houle, D., D.R. Govindaraju, and S. Omholt. 2010. Phenomics: the next challenge. Nature Rev.

764   Genetics 11:855-866.

765   Lorenz, A.J., S. Chao, F.G. Asoro, E.L. Heffner, R. Hayashi, H. Iwata, K.P. Smith, M.E. Sorrells,

766   and J-L. Jannink. 2011. In: L.S. Donald editors, Advances in Agronomy. Academic Press, The

767   Netherlands. p. 110:77-123.

768   Marjoram, P., A. Zubair, and S.V. Nuzhdin. 2014. Post-GWAS: where next? More samples, more

769   SNPs or more biology? Heredity 112: 79-88.

770   Messina, C.D., J.W. Jones, K.J. Boote, and C.E. Vallejos. 2006.A gene-based model to simulate

771   soybean development and yield responses to environment. Crop Sci. 46: 456-466.

772   Messina, C, G. Hammer, Z. Dong, D. Podlich, and M. Cooper. 2009. Modelling crop

773   improvement in a G*E*M framework via gene-trait-phenotype relationships. In: V.O. Sadras and

774   D. Calderini, editors, Crop physiology: applications for genetic improvement and agronomy.

775   Elsevier, The Netherlands. p. 235–265.

776   Messina, C.D., D. Podlich, Z. Dong, M. Samples, and M. Cooper. 2011. Yield-Trait performance

777   landscapes: from theory to application in breeding maize for drought tolerance. J. Exp. Bot. 62:

778   855-868.

779   Messina, C.D., T.R. Sinclair, G.L. Hammer, D. Curan, J. Thompson, Z. Oler, C. Gho, and M.

780   Cooper. 2015. Limited-Transpiration trait may increase maize drought tolerance in the US Corn

781   Belt. Agron. J. 107:1978-1986.

782   Meuwissen, T.H.E, B.J. Hayes, and M.E. Goddard. 2001. Prediction of total genetic value using

783   genome-wide dense marker maps. Genetics 157: 1819-1829.

784   Montana, G. 2005. HapSim: a simulation tool for generating haplotype data with pre-specified

785   allele frequencies and LD coefficients. Bioinformatics 21:4309-4311.

786   Monteith, J.L., and H. Unsworth. 1990. Principles of Environmental Physics. 2nd ed.

787   Butterworth-Heinemann, Jordan Hill, Oxford.

788   Muchow, R.C., T.R. Sinclair, and J.M. Bennett. 1990. Temperature and solar radiation effects on

789   potential maize yield across locations. Agron. J. 82: 338-343.

790   Muchow, R.C., and T.R. Sinclair. 1991. Water deficit effects on maize yields modeled under

791   current and "greenhouse"climates. Agron. J. 83: 1052-1059.

792   Pauli, D., S.C. Chapman, R. Bart, C.N. Topp, C.J. Lawerence-Dill, J. Poland, and M.A. Gore.

793   2016. The quest for understanding phenotypic variation via integrated approaches in the field

794   environment. Plant Physiol. 172:622-634.

795   Plummer, M., N. Best, K. Cowles and K. Vines. 2006. CODA: Convergence diagnosis and output

796   analysis for MCMC. *R News* 6:7-11.

797   R Core Team. 2014. R: A Language and Environment for Statistical Computing. Vienna, Austria:

798   R Foundation for Statistical Computing.

799   Reyes, A., C.D. Messina, G.L. Hammer, L. Liu, E. van Oosterom, R. Lafitte, M. Cooper. 2015.

800   Soil water capture trends over 50 years of single cross maize (Zea mays L.) breeding in the U.S.

801   corn-belt. J. Exp. Bot. 66:7339-7346.

802   Robertson, M.J., S. Fukai, M.M. Ludlow, and G.L. Hammer. 1993. Water extraction by grain

803   sorghum in a sub-humid environment. I. Analysis of the water extraction pattern. Field Crops

804   Res. 33:81–97.

805   Shekoofa, A., T.R. Sinclair, C.D. Messina, and M. Cooper. 2015 Variation among maize hybrids

806   in response to high vapor pressure deficit at high temperatures. Crop Sci. 55:392–396.

807   Sinclair, T. R., J.M. Bennett, and R.C. Muchow. 1990. Relative Sensitivity of Grain Yield and

808   Biomass Accumulation to Drought in Field-Grown Maize. Crop Sci. 30: 690-693.

809   Sinclair TR, and R.C. Muchow. 1999. Radiation Use Efficiency. In: L.S. Donald editors,

810   Advances in Agronomy. Academic Press, The Netherlands. p. 215-265.

811   Sinclair, T.R., and R.C. Muchow. 2001. System analysis of plant traits to increase grain yield on

812   limited water supplies. Agron. J. 93:263-270.

813   Sinclair, T.R., G.L. Hammer, and E.J. van Oosterom. 2005. Potential yield and water-use

814   efficiency benefits in sorghum from limited maximum transpiration rate. Funct. Plant Biol.

815   32:945-952.

816   Soltani, A., and T.R. Sinclair. 2012. Modeling physiology of crop development, growth and yield.

817   CAB International, Wallingford, UK.

818   Tanner, C.B., and T.R. Sinclair. 1983. Efficient water use in crop production: Research or re-

819   search? In: H. M. Taylor and W. R. Jordan, editors, Limitations to Efficient Water Use in Crop

820   Production. ASA, CSSA, and SSSA, Madison, WI. p. 1-27.

821   Technow, F., T. A. Schrag, W. Schipprack, and A. E. Melchinger. 2014a. Identification of key

822   ancestors of modern germplasm in a breeding program of maize. Theor. Appl. Genetics

823   127:2545–53.

824   Technow, F., T. A. Schrag, W. Schipprack, E. Bauer, H. Simianer, and A. E. Melchinger. 2014b.

825   Genome properties and prospects of genomic prediction of hybrid performance in a breeding

826   program of maize. Genetics 197:1343–55.

827   Technow, F., C.D. Messina, L.R. Totir, and M. Cooper. 2015. Integrating crop growth models

828   with whole genome prediction through approximate Bayesian computation. PLoS ONE 10(6):

829   e0130855.doi:10.1371/journal.pone.0130855

830   U.S. Department of Agriculture. 2015. Soil survey staff, Natural Resources Conservation Service,

831   United States Department of Agriculture. Web Soil Survey. [Online]. Available at

832   http://websoilsurvey.nrcs.usda.gov/. (Verified 7 March 2015)

833   Van Eeuwijk, F.A., M. Cooper, I.H. DeLacy, S. Ceccarelli, S., and S. Grando. 2001. Some

834   vocabulary and grammar for the analysis of multi-environment trials, as applied to the analysis of

835   FPB and PPB trials. Euphytica 122: 477-490.

836   Wallach, D., N. Keussayan, F. Brun, B. Lacroix, and J-E. Bergez. 2012. Assessing the uncertainty

837   when using a model to compare irrigation strategies. Agron. J. 104 :1274-1283.

838   Welcker, C., B. Boussuge, C. Bencivenni, J-M. Ribaut, and F. Tardieu. 2007. Are source and sink

839   strengths genetically linked in maize plants subjected to water deficit? A QTL study of the

840   responses of leaf growth and of anthesis-silking interval to water deficit. J. Exp. Bot. 58:339-349.

841   Yang, W., and R. J. Tempelman. 2012. A Bayesian antedependence model for whole genome

842   prediction. Genetics 190: 1491–1501.

843   Yin, X., P.C. Struik, and M.J. Kropff . 2004. Role of crop physiology in predicting gene-to-

844   phenotype relationships. Trends Plant Sci 9: 426-432.

845

846   Tables

847

848   Table 1. Mean prediction accuracies (± standard deviation) for yield estimated by the correlation

849   coefficient *r* for CGM-WGP prediction methodology and the reference method BayesA.

Estimation environment	Prediction environment					
	CGM-WGP			BayesA		
	WL1	WL2	NWL	WL1	WL2	NWL
WL1(1988)	0.85 ±0.03	0.51±0.13	0.60±0.13	0.84 ±0.03	0.38±0.17	-0.62±0.14
WL2(2012)	0.34±0.43	0.79±0.06	0.23±0.42	0.44±0.14	0.78±0.06	0.06±0.28
NWL(2010)	0.57±0.11	0.22±0.16	0.88±0.02	-0.60±0.11	0.01±0.26	0.88±0.02

850

851   Table 2. Mean prediction accuracies (± standard deviation) for yield estimated by the correlation

852   coefficient *r* for CGM-WGP prediction methodology and the reference methodBayesA and nine

853   cases defined by a unique combination of two or three environments utilized to train the

854   algorithms and one environment of utilized for evaluation of accuracy. Environments include two

855   water limited (WL) and one not water limited (NWL) conditions.

Estimation environment	Prediction environment					
	WL1(1988)	WL2(2012)	NWL(2010)	WL1(1988)	WL2(2012)	NWL(2010)
	--------- CGM-WGP ---------			--------- BayesA --------		
WL1 + WL2	0.79±0.04	0.75±0.05	0.67±0.08	0.77±0.04	0.51±0.13	-0.50±0.15
WL2 + NWL	0.72±0.09	0.75±0.06	0.81±0.04	-0.39±0.16	0.26±0.25	0.75±0.07
WL1 + WL2 + NWL	0.76±0.05	0.71±0.06	0.77±0.04	0.43±0.13	0.53±0.11	-0.01±0.2

856

857 Table 3. Mean prediction accuracies (± standard deviation) estimated by the correlation

858 coefficient *r* for physiological process parameters: size of the largest leaf within the leaf area

859 profile (AMAX), mass of ear at silking (MEB), radiation use efficiency (RUE) and limited

860 transpiration trait breakpoint (BKP).

Estimation environment	Physiological process parameter			
	AMAX	MEB	RUE	BKP
	----cm^{-2}----	----g----	----g MJ^{-1}----	-----kPa----
WL1 (1988)	0.31±0.16	0.52±0.15	0.33±0.16	0.65±0.14
WL2 (2012)	0.26±0.2	0.17±0.2	0.33±0.29	0.68±0.23
NWL (2010)	0.51±0.13	-0.03±0.19	0.66±0.13	0.17±0.21

861

862 Table 4. Mean prediction accuracies (± standard deviation) estimated by the correlation

863 coefficient *r* for physiological process parameters: size of the largest leaf within the leaf area

864 profile (AMAX), mass of ear at silking (MEB), radiation use efficiency (RUE) and limited

865 transpiration trait breakpoint (BKP).

Estimation environment	Physiological process parameter			
	AMAX	MEB	RUE	BKP
	----cm^{-2}----	----g----	----$g\ MJ^{-1}$----	-----kPa----
WL1 + NWL (1988 & 2010)	0.43±0.14	0.53±0.12	0.65±0.09	0.58±0.12
WL1 + WL2 (1988 & 2012)	0.42±0.10	0.46±0.14	0.51±0.11	0.78±0.07
WL2 + NWL (2012 & 2010)	0.47±0.11	0.28±0.18	0.66±0.10	0.77±0.07
WL1 + WL2 + NWL (1988 & 2010 & 2012)	0.44±0.12	0.51±0.12	0.60±0.08	0.75±0.07

866

867   Table 5. Estimates of the genetic correlation between the non-water-limited (NWL) and water-

868   limited (WL) environments ($r_{G(NWL,WL)} \pm$ Standard Error), genetic variance component within the

869   non-water-limited environment ($VG_{NWL} \pm$ Standard Error) and genetic variance component within

870   the water limited environment ($VG_{WL} \pm$ Standard Error) for grain yield (t ha^{-1}) of four DH

871   populations tested under WL and NWL environments at the DuPont Pioneer Viluco research

872   station in 2012.

DH Population	$r_{G(NWL,WL)}$	VG_{NWL}	VG_{WL}
DHPop1	-0.08 ± 0.19	0.515 ± 0.143	0.505 ± 0.130
DHPop2	-0.20 ± 0.17	0.686 ± 0.157	0.375 ± 0.103
DHPop3	0.36 ± 0.13	0.689 ± 0.161	1.433 ± 0.264
DHPop4	0.49 ± 0.11	0.944 ± 0.179	0.920 ± 0.168

873

874   Table 6. Average prediction accuracy for the CGM-WGP and BayesA methodologies obtained

875   from applying the leave-one-family-out cross-validation approach to prediction of grain yield

876   within the non-water-limited (NWL) and water-limited (WL) environments for four DH families.

DH family	CGM-WGP		BayesA	
	WL	NWL	WL	NWL
DHPop1	0.28	0.16	0.16	0.30
DHPop2	0.44	0.38	0.29	-0.06
DHPop3	0.64	0.21	0.50	0.29
DHPop4	0.45	0.18	0.36	0.02

877

878   Figures captions

879

880   Figure 1. Hierarchical crop growth model (CGM) whole genome prediction (WGP) algorithm.

881   Figure 2. Water supply to demand ratios estimated on a daily time step for Johnston, IA

882   calculated for 1988 (water limited, WL1) and 2012 (water limited 2, WL2) using a crop growth

883   model as a function of day of year. Simulated shedding dates for 1988 and 2012 indicated as

884   vertical bars. Model parameters were set to means of values utilized in sensitivity analyses, size

885   of the largest leaf in the leaf area profile (AMAX)=950, ear size at silking (MEB)=0.8, radiation

886   use efficiency (RUE)=1.8, and limited transpiration breakpoint (BKP)=2.25

887   Figure 3. Response of standardized yield to variation in crop growth model parameters: (a) size of

888   the largest leaf in the leaf area profile (AMAX, cm^2), (b) ear size at silking (MEB, g), (c)

889   radiation use efficiency (RUE, g MJ^{-1}), and (d) limited transpiration breakpoint (BKP, kPa) for

890   water limited environments (WL1) 1988 and (WL2) 2010, and not water limited environment

891   (NWL) 2012 at Johnston, IA USA (See Figure 2 for dynamics in supply/demand ratio). Yields

892   were standardized relative to the overall mean (1054 g m^{-2}) and standard deviation (407 g m^{-2}).

893   Figure 4. Water supply to demand ratios for DuPont Pioneer Viluco research station in 2012

894   calculated for water limited (WL) and not water limited (NWL) conditions using a crop growth

895   model as a function of day of year. Simulated shedding date for NWL and WL treatments

896   indicated as closed and open squares. Model parameters were set to means of values utilized in

897   sensitivity analyses, size of the largest leaf in the leaf area profile (AMAX)=950, ear size at
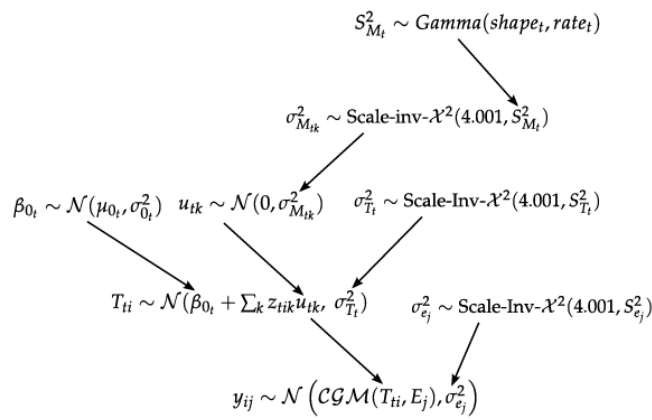
898   silking (MEB)=0.8, radiation use efficiency (RUE)=1.8, and limited transpiration breakpoint

899   (BKP)=2.25

900   Figure5. Grain yield observed under water-limited at flowering (WL) and non-water-limited

901   (NWL) due to well watered (WW) environmental conditions for four DH families evaluated at

902   the DuPont Pioneer Viluco research station in 2012.

903   Figure 6. Simulated yields for the major maize growing regions in the U.S. corn belt for 2014

904   (a,b) and 1988 (a,c) and individuals of a breeding population with CGM parameters estimated

905   from maker data using the CGM-WGP methodology.

906   Figure 1

$$S^2_{M_t} \sim Gamma(shape_t, rate_t)$$

$$\sigma^2_{M_{tk}} \sim \text{Scale-inv-}\mathcal{X}^2(4.001, S^2_{M_t})$$

$$\beta_{0_t} \sim \mathcal{N}(\mu_{0_t}, \sigma^2_{0_t}) \quad u_{tk} \sim \mathcal{N}(0, \sigma^2_{M_{tk}}) \quad \sigma^2_{T_t} \sim \text{Scale-Inv-}\mathcal{X}^2(4.001, S^2_{T_t})$$

$$T_{ti} \sim \mathcal{N}(\beta_{0_t} + \sum_k z_{tik} u_{tk}, \sigma^2_{T_t}) \quad \sigma^2_{e_j} \sim \text{Scale-Inv-}\mathcal{X}^2(4.001, S^2_{e_j})$$

$$y_{ij} \sim \mathcal{N}\left(\mathcal{CGM}(T_{ti}, E_j), \sigma^2_{e_j}\right)$$

Observed data

y_{ij} – yield of individual i in environment j

E_j – specifications for environment j

z_{tik} – score of individial i at marker k of trait t

Unobserved parameters

T_{ti} – biological trait t of individual i

β_{0_t}, u_{tk} – intercept and effect of marker k for trait t
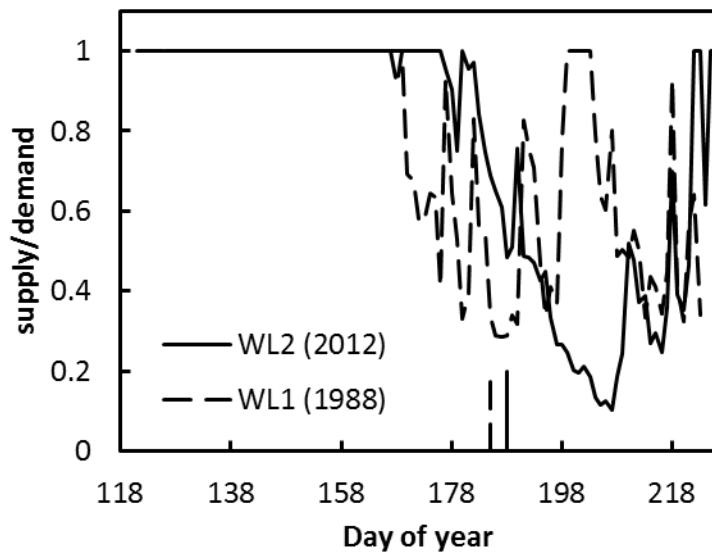
μ_{0_t} – prior mean of β_{0_t}

$\sigma^2_{e_j}, \sigma^2_{T_t}, \sigma^2_{M_{tk}}, \sigma^2_{0_t}$ – residual yield variance in env. j, prior variances of traits, marker effects, and intercepts

$S^2_{e_j}, S^2_{T_t}, S^2_{M_t}$ – scale parameters of priors for residual yield variance, variance of trait t and of marker effects

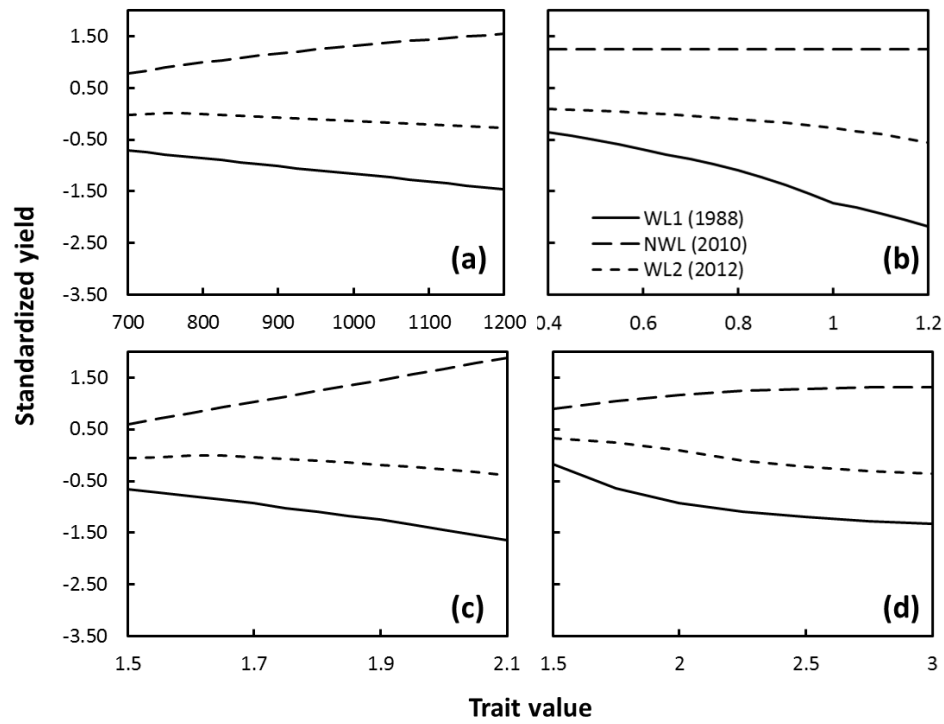$shape_t, rate_t$ – parameters for prior of $S^2_{M_t}$

907

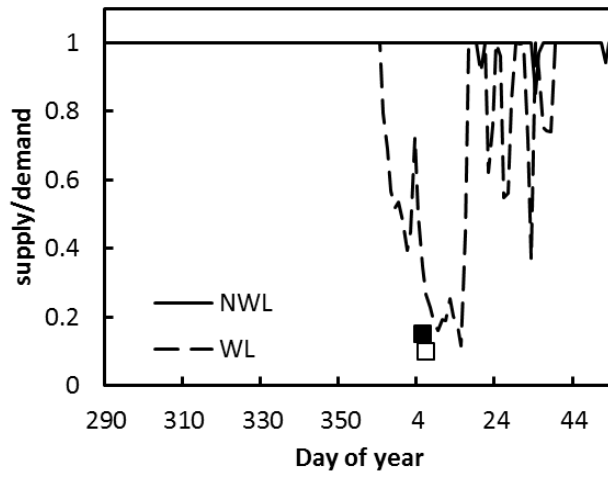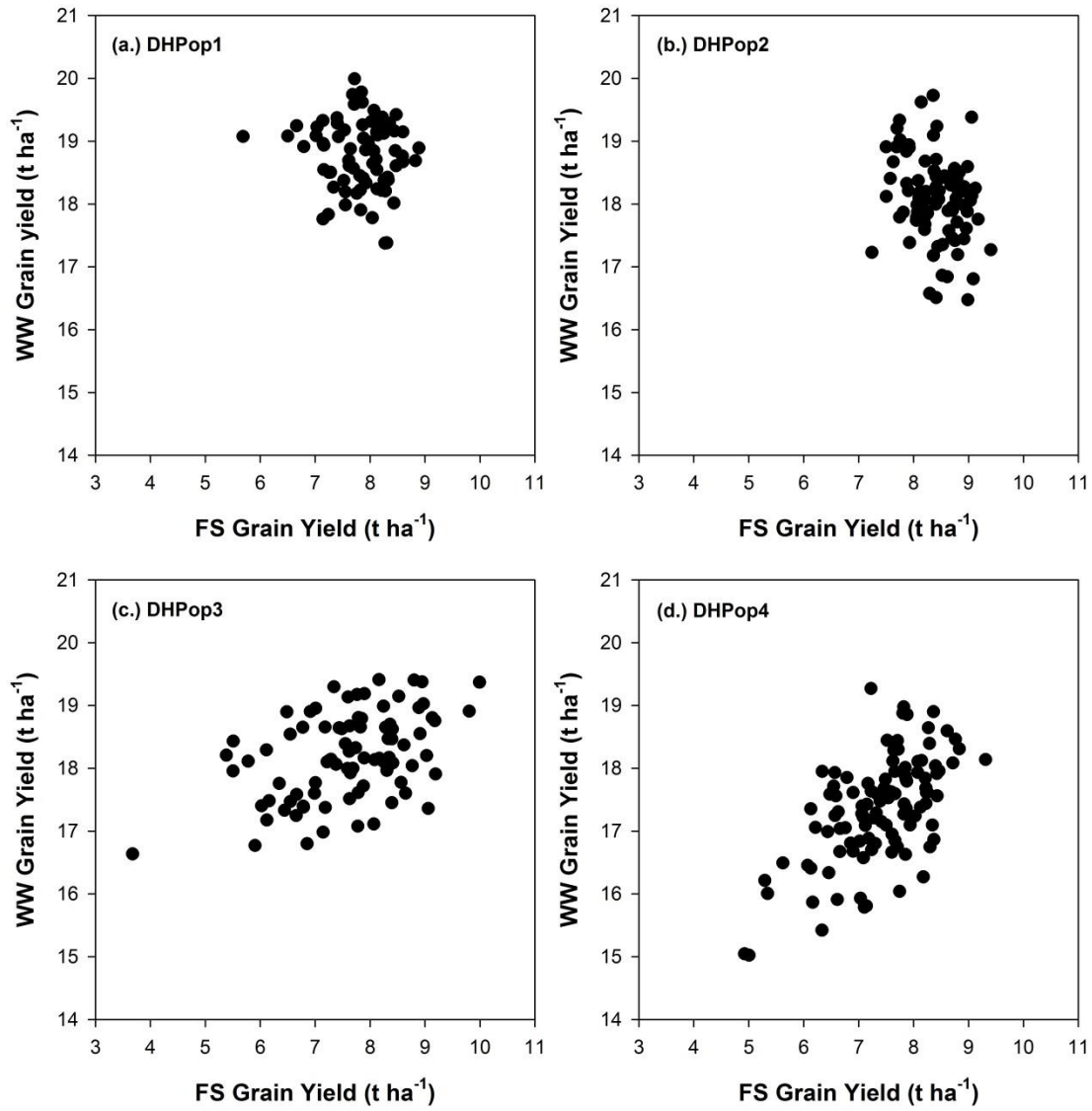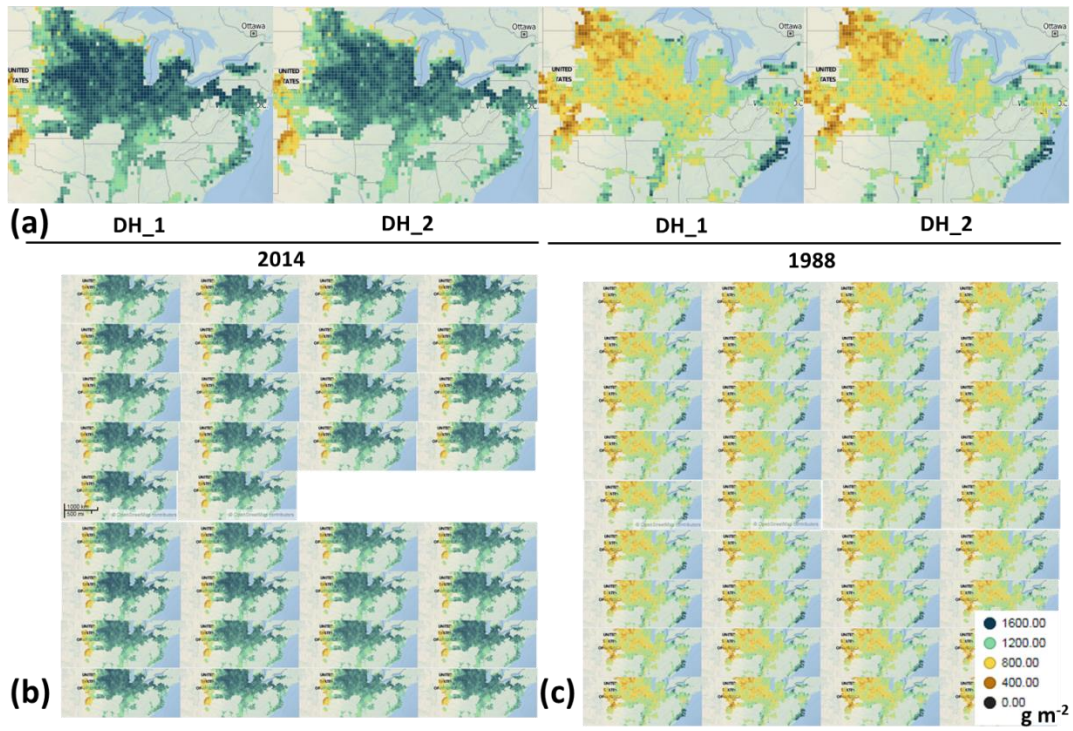908   Figure 2

909

910   Figure 3

911

912   Figure 4

913

914   Figure 5

915

916   Figure 6

917